Available online at www.sciencedirect.com
SCIENCE DIRECT®
International Journal of Heat and Mass Transfer 48 (2005) 3185–3196
International Journal of HEAT and MASS TRANSFER
www.elsevier.com/locate/ijhmt

Dynamic performance of a natural circulation loop with end heat exchangers under different excitations

N.M. Rao [a,*], B. Maiti [b], P.K. Das [b]

[a] Department of Mechanical Engineering, Dr. Babasaheb Ambedkar Technological University, 'Vidyavihar', Lonere 402 103, Maharashtra State, India
[b] Department of Mechanical Engineering, Indian Institute of Technology, Kharagpur 721 302, West Bengal, India

Received 11 August 2004; received in revised form 28 January 2005

Abstract

In the present work the dynamic performance of a natural circulation loop (NCL) has been studied under step, ramp, exponential and sinusoidal excitations. The loop is equipped with two heat exchangers at its lower and upper end for the heating and cooling of the loop fluid. For the analysis, transient one-dimensional conservation equations have been constructed for the loop fluid as well as for the two fluid streams of hot and cold end heat exchangers. The solution of a set of differential equations and one integro-differential equation has been obtained through a finite element method (FEM). For different excitations imposed to the inlet temperature of the hot fluid responses have been studied for the outlet temperature of the two fluid streams and the mass flow rate of the coupling fluid. It has been observed that all these quantities experience some initial transients before reaching the steady state. Time needed for the attainment of steady state varies with the type of excitation. A finite time delay is observed before the cold fluid stream temperature starts responding to the excitation. This delay is related to the time required for the advection of a fluid particle.

Keywords: Dynamic response; Natural circulation loop; Finite element method; End heat exchangers; Inlet excitations

1. Introduction

The transient behaviour of natural circulation loop (NCL) is a subject of investigation for a variety of reasons. In a forced circulation loop (FCL) flow field develops due to the action of the prime-mover. Such loops may exhibit transient behaviour during startup, shutdown, flow control and accident. However, for single phase FCLs such transients are short lived and may not lead to substantial deviation from the steady state behaviour. If a mixture of two phases passes through FCL these oscillations get augmented and sometimes becomes detrimental to the safe operation of the system. On the other hand, in an NCL the loop fluid flow is driven by thermally generated density gradient so that a pump is not required. The generation of density gradient is caused by temperature variations of fluid due to simultaneous heating and cooling at different parts of the

* Corresponding author. Tel.: +91 2140 275228(R); fax: +91 2140 275040.
E-mail addresses: nmuralidhararao@yahoo.com (N.M. Rao), bmaiti@mech.iitkgp.ernet.in (B. Maiti), pkd@mech.iitkgp.ernet.in (P.K. Das).

0017-9310/$ - see front matter © 2005 Elsevier Ltd. All rights reserved.
doi:10.1016/j.ijheatmasstransfer.2005.02.022

Nomenclature

A_s	cross-sectional area, m^2
c	specific heat, kJ/kg K
C	heat capacity rate, kW/K
C^*	non-dimensional heat capacity rate, $\left(\frac{C}{(\mu cD)_{cf}}\right)$
C_f	friction factor, dimensionless
$C^*_{max,c}$	larger heat capacity rate of the fluid in CEHE side, dimensionless
$C^*_{max,h}$	larger heat capacity rate of the fluid in HEHE side, dimensionless
$C^*_{min,c}$	smaller heat capacity rate of the fluid in CEHE side, dimensionless
$C^*_{min,h}$	smaller heat capacity rate of the fluid in HEHE side, dimensionless
CR^*_c	$C^*_{min,c}/C^*_{max,c}$ (cold fluid side), dimensionless
CR^*_h	$C^*_{min,h}/C^*_{max,h}$ (hot fluid side), dimensionless
D	loop diameter, m
g	gravitational acceleration, m/s^2
Gr_L	loop Grashof number, dimensionless, $\left(\frac{\rho_0^2 g\beta D^3(T_0-T_{ci})}{\mu_{cf}^2}\right)$
L_1	horizontal length of the loop, m
L_2	vertical length of the loop, m
Ntu_c	$(UA)_c/C_{min,c}$ (CEHE), dimensionless
Ntu_h	$(UA)_h/C_{min,h}$ (HEHE), dimensionless
Ntu^*_c	$(UA)^*_c/C^*_c$
Ntu^*_h	$(UA)^*_h/C^*_h$
P	pressure, kN/m^2
Re	Reynolds number, $(\rho uD/\mu)_{cf}$
s	space coordinate, m
S	non-dimensional space coordinate, $(\frac{s}{L_1})$
t	time, s
T	temperature, K
u	velocity, m/s
UA	product of over-all heat transfer coefficient and heat transfer area, kW/K
$(UA)^*$	non-dimensional product of over-all heat transfer coefficient and heat transfer area, $\left(\frac{(UA)}{(\mu cD)_{cf}}\right)$

Greek symbols

β	thermal expansion coefficient, K^{-1}
ε^*	effectiveness
θ	non-dimensional temperature, $\left(\frac{(T-T_{ci})}{(T_0-T_{ci})}\right)$
μ	viscosity, kg/m s
ρ	density, kg/m^3
τ	non-dimensional time, dimensionless, $(t[(\frac{\mu D}{\rho A_s})_{cf}\frac{1}{L_1}])$
ϕ	angle of inclination

Subscripts

c	cold stream
cf	coupling fluid
cf1	steady state (downcomer)
cf2	steady state (riser)
cfs	spatial variation of coupling fluid
cfss	steady state coupling fluid
ci	cold stream inlet
co	cold stream outlet
cs	spatial variation of cold fluid
d	delay
hi	hot stream inlet
ho	hot stream outlet
hs	spatial variation of hot fluid
0	reference

loop. The loops are often heated from below and cooled from the above, which then establishes a stable density gradient in the fluid. Under the influence of gravitational force the lighter fluid rises and heavier fluid falls. Under the stable operation of the loop the fluid experiences a continuous unidirectional flow through the loop. As these loops do not require any auxiliary power they can be designed as highly reliable and self-contained systems. Since, the flow and temperature fields are interdependent and the operator or the designer does not have a direct control over the circulation rate even under the steady state condition. This feature makes the NCL susceptible to oscillations during the startup, shutdown, emergency or accidental scenario and process control operation. Earlier investigations on NCLs illustrated many aspects of the flow and heat transfer including the presence of reverse flows and oscillations. Oscillatory flow delays the attainment of the steady state in general and in some extreme cases may lead to catastrophic situations. Flow reversals and flow stagnation can cause undesirable increase of localized temperature and even causes damage to the system. Moreover, the dynamic response of a NCL with heat exchangers may be used for the system identification and determination of system characteristics in varied engineering applications, ranging from low capacity boilers and micro-coolers to large nuclear power plants and space heat sinks.

Though, the dynamic behaviour of NCLs has been studied for different loop configurations and various heat transfer arrangements, single phase rectangular NCL with end heat exchangers has not yet been considered. However, Rao et al. [1–3] studied the steady state performance of a rectangular NCL with end heat exchangers, its total and dynamic pressure variation under steady state and transient conditions and its stability behaviour, respectively. Systems such as NCLs with end

heat exchangers can be termed as fluid coupled indirect heat exchange systems where the circulation of the coupling fluid is achieved by exploiting the buoyancy force. The theory of liquid coupled indirect heat exchanger systems (FCLs) has been studied by Holmberg [4]. In his study he ascertained the optimum criteria with respect to the coupling fluid flow rate and the distribution of total heat transfer area between the hot side and cold side exchanger units especially in case of counterflow arrangement.

Recently, Luo et al. [5] modelled and simulated the dynamic behaviour of one-dimensional flow (co-current and countercurrent) multistream heat exchangers and their networks. They have introduced four connection matrices through which the solution becomes general and it could directly be applied to one-dimensional flow heat exchanger networks. The responses to inlet temperature and flow rate variations are calculated numerically and for some cases analytically. Examples have taken to illustrate the procedure. One of these is indirect coupled heat exchanger system where, for the circulation of coupling fluid a prime-mover is used. A most general analytical calculation method is presented for systems of counterflow and co-currentflow heat exchangers by Ranong and Roetzel [6]. They further, extended this method to the FCL system of two coupled heat exchangers.

On the other hand, extensive studies have been made on the dynamic behaviour of direct heat exchange systems or conventional heat exchangers having different fluid flow arrangements namely, parallel, countercurrent and cross. Heggs and Render [7] reported the transient response of heat exchangers with one infinite capacitance fluid for the step change in inlet temperature. However, Romie [8] investigated the exit fluid temperature responses of a counterflow heat exchanger for a unit step increase in the inlet temperature of either of fluid streams with finite heat capacitance of fluids. In another study similar investigations have been done by Romie [9] for the parallel-flow heat exchanger. The transient response of gas–gas parallel and countersss flow heat exchangers has been reported by Gvozdenac [10]. A complete parametric study has been carried out by Pagliarini and Barozzi [11] on the thermal interaction between the streams of laminar flow in double-pipe heat exchangers accounting for axial conduction along the wall, separating the fluids. Roetzel and Xuan [12] formulated a method using Laplace transform for both parallel and counterflow heat exchangers. The exit temperature responses have been calculated for step and sinusoidal inlet temperature changes. Roetzel and Xuan [13] also focused their study to predict the transient exit temperature responses for step, ramp, exponential and sinusoidal inlet temperature changes for a multi-pass shell and tube heat exchangers. Further, they [14] studied the effect of longitudinal heat conduction in the wall core as well as the thermal capacities of both fluids and the wall to predict the transient exit temperature responses of counterflow heat exchanger for both step and sinusoidal change in inlet temperatures. An analytical and experimental transient response of temperatures along the length of the counterflow heat exchanger has been reported by Abdelghani-Idrissi et al. [15] when a step change in hot liquid flow rate was applied. The influence of initial and final flow rates and the transient response to positive and negative flow rate step were presented.

In the present investigation the dynamic behaviour of NCLs with end heat exchangers have been studied. A schematic diagram of the system is given in Fig. 1. The natural circulation system is idealized as a vertical rectangular loop with constant cross-sectional area. The hot end heat exchanger (HEHE) is located at the bottom of the loop while the cold end heat exchanger (CEHE) is at the top as depicted in Fig. 1. The working of the loop at steady state is as follows. Four prominent zones can be identified in the loop. The coupling fluid enters the bottom section (M–N) with a temperature T_{cf1} and density ρ_{cf1}. The fluid gets heated up while passing through the hot end heat exchanger by absorbing heat from the hot stream and leaves with temperature and density T_{cf2} and ρ_{cf2} ($T_{cf2} > T_{cf1}$ and $\rho_{cf2} < \rho_{cf1}$), respectively. The lighter fluid ascends through the adiabatic riser (N–O) without changing its density. While flowing through the top section (O–P) the coupling fluid rejects heat to the cold stream and finally attains a temperature T_{cf1}. A

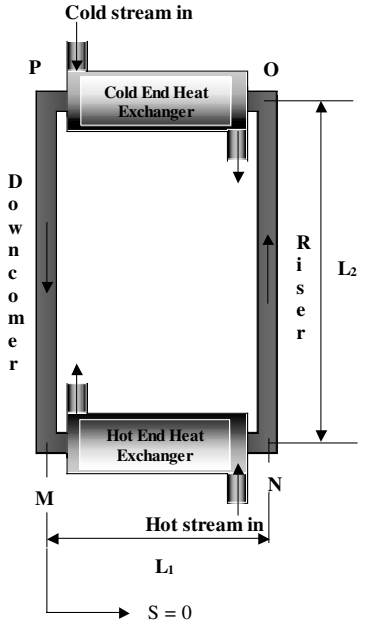

Fig. 1. Schematic diagram of a single phase NCL with end heat exchangers.

downward flow of the coupling fluid through the adiabatic downcomer (P–M) completes the circulation loop.

2. Theoretical analysis

For exploring the dynamic behaviour of the NCL with end heat exchangers a known temperature perturbation is given to the inlet of the HEHE and the response of the system is studied. The excitations such as step, modified ramp, modified exponential and sinusoidal for hot stream inlet temperature have been considered for the dynamic response of the system.

The analysis is made based on the following assumptions:

- The hot and cold stream heat capacity rates remain constant.
- The over-all heat transfer coefficients and the surface area per unit length for the heat exchangers are constant throughout their length.
- The thermal properties of all the fluid streams are uniform and constant.
- There is no variation of temperature and velocity in a cross-sectional plane.
- Density of a coupling fluid is a linear function of its temperature.
- The density variation in the coupling fluid has been considered only in the body force term (Boussinesq approximation).
- Flow inside the loop is turbulent and the friction factor is a sole function of Reynolds number.
- The wall capacitance is neglected.
- No heat is conducted along the axial directions of the three fluids.
- Vertical limbs (riser and downcomer) are adiabatic.
- Minor losses due to bends and fittings have been neglected.

Based on the above idealizations following conservation equations may be written:

As the velocity depends only on time, the continuity equation may be written for the incompressible coupling fluid as

$$u_{cf} = u_{cf}(t). \tag{1}$$

The momentum equation for a differential fluid element inside the loop can be written as

$$\frac{\partial P}{\partial s} = -\left[\rho_{cf}\frac{\partial u_{cf}}{\partial t} + \rho_{cf} g \sin\phi + \frac{2C_f \rho_{cf} u_{cf}^2}{D}\right]. \tag{2}$$

One can now introduce a functional relationship between friction factor, C_f, and Reynolds number, Re, in the following form:

$$C_f = aRe^{-b} \tag{3}$$

where a and b are constants. Relationship of this form is valid over a wide range of Reynolds number covering both laminar and turbulent regions. However, the constants have different values for these two regions.

Incorporating the relationship for friction factor in the differential momentum equation, one gets,

$$\frac{\partial P}{\partial s} = -\left[\rho_{cf}\frac{\partial u_{cf}}{\partial t} + \rho_{cf} g \sin\phi + \frac{2a\mu_{cf}^b \rho_{cf}^{1-b}}{D^{1+b}} u_{cf}^{2-b}\right]. \tag{4}$$

The density variation in the body force term may be assumed a linear function of temperature [16–18]:

$$\rho_{cf} = \rho_0[1 - \beta(T_{cf} - T_0)]. \tag{5}$$

Integrating Eq. (4) around the loop and substitution of Eq. (5) in body force terms, one gets the momentum equation in an integral form.

$$\frac{2(L_1+L_2)}{(A_s c)_{cf}}\frac{\partial C_{cf}}{\partial t} + \frac{4a\mu_{cf}^b (L_1+L_2)}{\rho_{cf}(A_s c)_{cf}^{2-b}} C_{cf}^{2-b} + \rho_0 g\beta\left[\int_{(2L_1+L_2)}^{2(L_1+L_2)} T_{cf}\,ds - \int_{L_1}^{(L_1+L_2)} T_{cf}\,ds\right] = 0, \tag{6}$$

where C_{cf} is the coupling fluid heat capacity rate.

Energy balance for the hot stream and the coupling fluid can be derived considering a differential element (Δs) of HEHE of the NCL (Fig. 2a) in Eqs. (7) and (8):

$$\frac{\partial T_h}{\partial t} - u_h\frac{\partial T_h}{\partial s} + \frac{(UA)_h}{(\rho A_s c)_h L_1}(T_h - T_{cf}) = 0, \tag{7}$$

$$\frac{\partial T_{cf}}{\partial t} + u_{cf}\frac{\partial T_{cf}}{\partial s} + \frac{(UA)_h}{(\rho A_s c)_{cf} L_1}(T_{cf} - T_h) = 0. \tag{8}$$

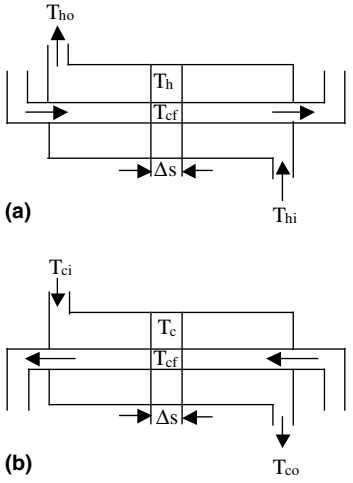

Fig. 2. Schematic diagrams of end heat exchanger: (a) hot end heat exchanger (HEHE) and (b) cold end heat exchanger (CEHE).

Similarly, the energy balance of the cold stream and the coupling fluid inside CEHE (Fig. 2b) can be expressed in Eqs. (9) and (10), respectively.

$$\frac{\partial T_c}{\partial t} - u_c \frac{\partial T_c}{\partial s} + \frac{(UA)_c}{(\rho A_s c)_c L_1}(T_c - T_{cf}) = 0, \tag{9}$$

$$\frac{\partial T_{cf}}{\partial t} + u_{cf} \frac{\partial T_{cf}}{\partial s} + \frac{(UA)_c}{(\rho A_s c)_{cf} L_1}(T_{cf} - T_c) = 0. \tag{10}$$

Energy equation can be written for the coupling fluid within a differential element (Δs) of the fluid in the adiabatic riser and downcomer in the following form:

$$\frac{\partial T_{cf}}{\partial t} + u_{cf} \frac{\partial T_{cf}}{\partial s} = 0. \tag{11}$$

As in the present study the excitation has been imposed at the inlet hot stream temperature, the boundary conditions become

$$T_h(s,t) = T_h(t) \quad \text{at } s = L_1, \text{ i.e., at a station '}\mathbf{N}\text{'}, \tag{12}$$

$$T_c(s,t) = T_{ci} \quad \text{at } s = (2L_1 + L_2), \text{ i.e., at a station '}\mathbf{P}\text{'}. \tag{13}$$

The initial conditions are

$$T_{h,c,cf}(s,0) = \text{constant(known temperature)} \quad \text{at } s = s \text{ and } t = 0. \tag{14}$$

Momentum and energy equations along with the boundary conditions can be non-dimensionalised by using the following substitutions:

$$C^*_{h,c,cf} = \frac{C_{h,c,cf}}{(\mu c D)_{cf}}, \tag{15a}$$

$$(UA)^*_{h,c} = \frac{(UA)_{h,c}}{(\mu c D)_{cf}}, \tag{15b}$$

$$\theta_{h,c,cf} = \frac{(T_{h,c,cf} - T_{ci})}{(T_0 - T_{ci})}, \tag{15c}$$

$$\tau = t\left[\left(\frac{\mu D}{\rho A_s}\right)_{cf} \frac{1}{L_1}\right], \tag{15d}$$

$$S = \frac{s}{L_1}, \quad K_1 = \frac{L_2}{L_1}, \quad K_2 = \frac{L_1}{D}, \tag{15e}$$

$$Ntu^*_{h,c} = \frac{(UA)^*_{h,c}}{C^*_{h,c}}, \tag{15f}$$

$$Gr_L = \frac{\rho_0^2 g \beta D^3 (T_0 - T_{ci})}{\mu_{cf}^2}. \tag{15g}$$

Using the above non-dimensional parameters, Eqs. (6)–(11) can be represented as (16)–(21), respectively:

$$\frac{\partial C^*_{cf}}{\partial \tau} + \frac{\pi^b a K_2}{2^{2b-1}}(C^*_{cf})^{2-b} + \frac{\pi^2}{2^5} Gr_L K_2 \times \frac{1}{(1+K_1)}\left[\int_{(K_1+2)}^{2(K_1+1)} \theta_{cf}\, dS - \int_1^{(K_1+1)} \theta_{cf}\, dS\right] = 0, \tag{16}$$

$$\frac{\partial \theta_h}{\partial \tau} - C^*_h R_h \frac{\partial \theta_h}{\partial S} + Ntu^*_h C^*_h R_h(\theta_h - \theta_{cf}) = 0, \tag{17}$$

$$\frac{\partial \theta_{cf}}{\partial \tau} + C^*_{cf} \frac{\partial \theta_{cf}}{\partial S} + Ntu^*_h C^*_h(\theta_{cf} - \theta_h) = 0, \tag{18}$$

$$\frac{\partial \theta_c}{\partial \tau} - C^*_c R_c \frac{\partial \theta_c}{\partial S} + Ntu^*_c C^*_c R_c(\theta_c - \theta_{cf}) = 0, \tag{19}$$

$$\frac{\partial \theta_{cf}}{\partial \tau} + C^*_{cf} \frac{\partial \theta_{cf}}{\partial S} + Ntu^*_c C^*_c(\theta_{cf} - \theta_c) = 0, \tag{20}$$

$$\frac{\partial \theta_{cf}}{\partial \tau} + C^*_{cf} \frac{\partial \theta_{cf}}{\partial S} = 0, \tag{21}$$

where $R_{h,c} = \frac{(\rho A_s c)_{cf}}{(\rho A_s c)_{h,c}}$ ratio of coupling fluid heat capacitance to hot/cold stream heat capacitance per unit length.

The boundary conditions become in non-dimensional form as

$$\theta_h(S,\tau) = \theta_h(\tau) \quad \text{at } S = 1.0, \tag{22a}$$

$$\theta_c(S,\tau) = 0.0 \quad \text{at } S = (K_1 + 2). \tag{22b}$$

The non-dimensional initial conditions are

$$\theta_{h,c,cf}(S,\tau) = 0.0 \quad \text{at } S = S \quad \text{and} \quad \tau = 0. \tag{22c}$$

Solution may be obtained for any arbitrarily chosen temperature function $\theta_h(\tau)$. However, for dynamic response of the loop, one is generally interested for step, ramp and exponential variation of temperature. Such variation may occur during operations or they may be especially created for the purpose of testing the loop under transient state. Though, a ramp or an exponential function gives a continuous increase in temperature, such an increase for a prolonged duration is not feasible in reality. For instance the initial temperature rise may have the ramp or exponential nature in both designed and unforeseen transients, but the maximum value of temperature rise will generally be limited. In the present study, instead of continuous increase, a limit has been imposed on maximum temperature rise, which is 1.0. Consideration of a ramp input with a limit on the maximum temperature is also important, as the realization of an ideal step input is not possible. In practice there will be a slope (whatever small it may be) of the temperature rise curve. Additionally sinusoidal input function has also been tried for the temperature responses. Accordingly the functional form of $\theta_h(\tau)$ is expressed as follows:

$$\theta_h(\tau) = \begin{cases} 1 \quad \text{for step input,} \\ \begin{bmatrix} \alpha\tau, & \tau \leqslant \alpha^{-1}, \\ 1, & \tau > \alpha^{-1} \end{bmatrix} \quad \text{for ramp input,} \\ 1 - e^{-\alpha\tau} \quad \text{for exponential input,} \\ [0.75 + (0.25 \sin \alpha\tau)] \quad \text{for sinusoidal input.} \end{cases} \tag{23}$$

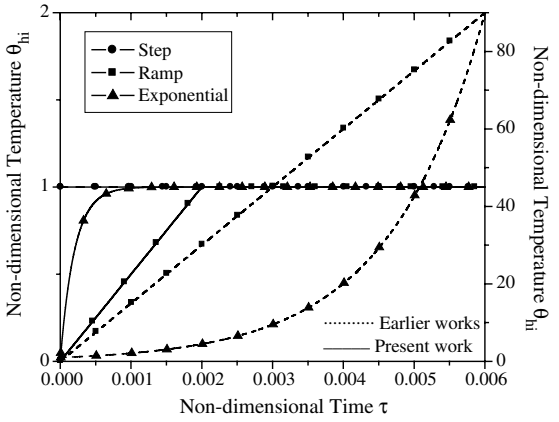

Fig. 3. Schematic representation of the input signals.

The input signals are schematically represented in Fig. 3. For the present study, α has been taken as 500 for ramp input and 5000 for exponential input. Two frequencies have been considered for the sinusoidal excitation. For the sinusoidal excitation the value of 'α' has been taken as 5000 for lower frequency and 15,000 for higher frequency.

3. Solution methodology

For the dynamic analysis one needs to solve Eqs. (16)–(21) in its full form. This cannot be done by any analytical technique. Finite element method (FEM) has been adopted to solve the momentum and energy equations in the transient state. The quadratic elements with two degrees of freedom (θ_{cf}, θ_h or θ_c) have been considered in the heat exchanger zones while the elements have single degree of freedom in the riser and downcomer (θ_{cf}). In the present case, the momentum and energy equations are coupled with each other and the system is having only two natural boundary conditions (hot and cold stream non-dimensional inlet temperatures). As the values of either the velocity or the temperature of the coupling fluid is not known any where in the loop at the beginning, an iterative guess-and-correct procedure has been used. To start with, a coupling fluid velocity in the loop and the temperature at any particular location of the loop (say 'S') is assumed. Due to continuity of temperature, the identical value of temperature should exist also at $[2(K_1 + 1) + S]$ moving in the same direction of the loop, where $2(K_1 + 1)$ is the total length of the loop. Further, the value of the coupling fluid velocity, if assumed correctly, should satisfy the loop momentum equation. These two criteria have been used for correcting the initial guesses of the temperature and coupling fluid velocity.

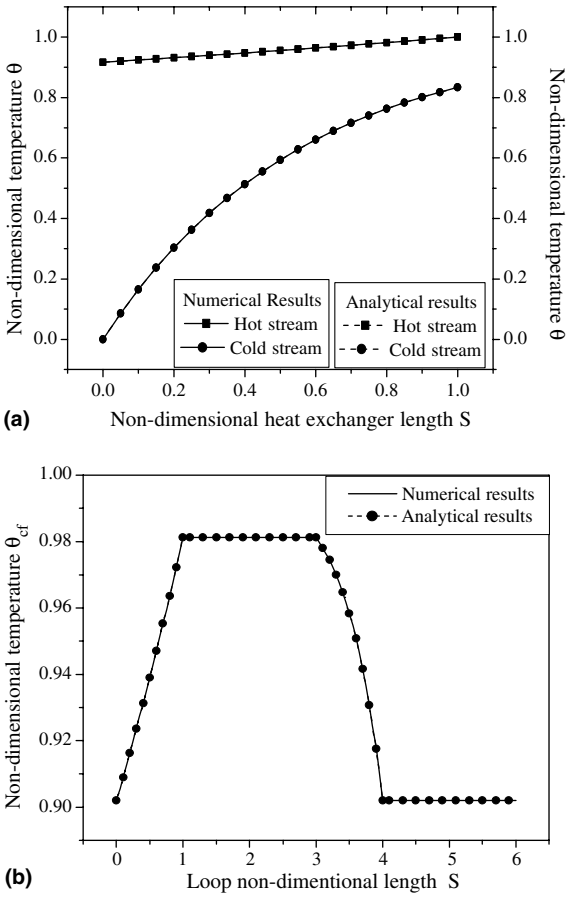

Fig. 4. Comparison between numerical and analytical results at steady state: (a) hot and cold stream temperature profile and (b) coupling fluid temperature profile.

The details of the finite element formulation and solution procedure are given in Rao [19].

To check the validity of this numerical technique, initially solution has been obtained for the steady state case. For this, step excitation of the inlet temperature of hot stream has been considered and the finite element program has been run for a sufficiently long time to get the solution of the coupled system. Results have been compared with those obtained from the analytical expressions of the steady state solution as obtained by Rao [19] and depicted in Fig. 4a and b. Finite element solutions exhibit excellent agreement with the analytical results.

4. Results and discussion

The results and their analysis are given below for specific step, ramp, exponential and sinusoidal excitations imposed at the inlet hot fluid temperature.

4.1. Step, ramp and exponential excitations

Dynamic response of the NCL for a step change of hot stream inlet temperature is considered first. A series of complex and coupled phenomena occur as a step input is provided at the inlet of the hot stream. Initially, the loop as well as the cold and the hot streams are at the same temperature (frozen state of the loop). This implies no temperature gradient along the loop and as a result no circulation is induced through it. With the imposition of step input the temperature field will develop along the loop length. This will induce a circulation through the loop. The circulation will, on the other hand, influence the development of the temperature field. This mutual interaction between the temperature field and fluid flow will continue till a steady state is reached. The temperature of the fluid streams changes with space and time, while the circulation rate changes with time. Therefore, the development of the thermo-fluid process in the system can be appreciated fully by studying the changes in both space and time. For the sake of clarity these are depicted graphically in Figs. 5 and 6. In Fig. 5 the temporal changes of the exit temperatures of the two streams (θ_{ho} and θ_{co}) and the circulation rate (C^*_{cf}) are depicted from the inception of transient till the attainment of the steady state, whereas, in Fig. 6 the variation of coupling fluid temperature over the loop length has been shown for discrete time steps. In Fig. 6 the total loop length has been divided into four parts namely, MN, NO, OP and PM representing the HEHE, riser, CEHE and downcomer, respectively.

Initially, as there is small flow through the loop the coupling fluid inside the HEHE will be heated almost at stagnant condition. As the rate of heat removal from the hot stream is rather low, the exit temperature of the hot stream will rise very rapidly. The temperature rise at the hot stream exit will closely follow the step input imposed at its inlet. The hot stream exit temperature will eventually reach a maximum value marginally lower than the step input. This is depicted in Fig. 5 and the maximum value is denoted as *A* in the hot stream exit temperature.

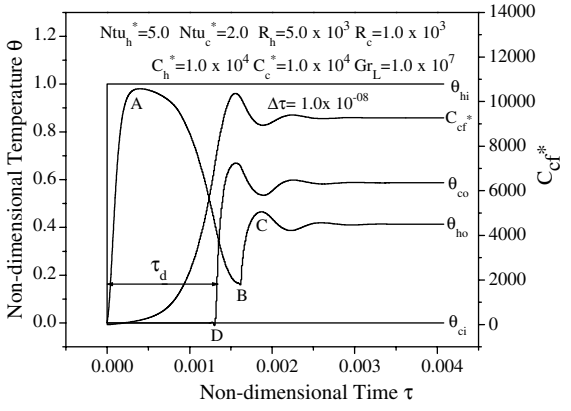

Fig. 5. Exit responses of hot and cold stream to step change in hot stream inlet temperature.

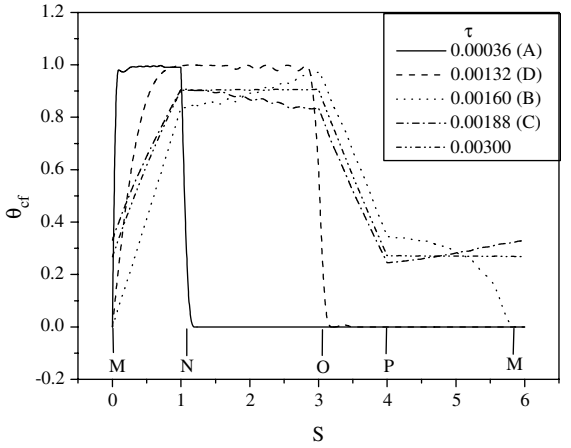

Fig. 6. Temporal development of temperature profile of coupling fluid along the loop length.

To investigate the associated development of temperature field in the loop, the loop temperature profiles at different time steps have been recorded. They are shown in Fig. 6. The temperature profile corresponding to point *A* shows a high value of coupling fluid temperature throughout the length of the HEHE, but a low uniform value elsewhere in the loop. As the two vertical limbs of the loop are almost at the same temperature, there is negligible flow through the loop. This is also supported by the variation of C^*_{cf} with time depicted in Fig. 5. Gradually, small circulation will set inside the loop. The hot stream exit temperature will start declining after its attainment of the maximum temperature. Initially, the rate of decline of the exit temperature is rather low, but as the mass flow rate increases, the exit temperature decreases at a faster rate. The lowest value of the hot stream exit temperature is at *B*. Interestingly, this is lower than the steady state value of the hot stream exit temperature. Explanation of this phenomenon may be obtained from the loop temperature curve at $\tau = 0.0016$ given in Fig. 6. NO and PM in the curve denote the temperature variation in the riser and the downcomer, respectively. The higher the difference in temperature in these two portions, the larger is the circulation rate. In the temperature curve corresponding to $\tau = 0.0016$, it is observed clearly that the temp difference between the riser and downcomer is the largest denoting maximum rate of circulation. This also corresponds to the peak of the C^*_{cf} curve in Fig. 5. As the circulation velocity is maximum the hot stream exit temperature will be minimum due to high rate of heat removal. Beyond

this point the downcomer temperature will start rising whereas there is a decrease in riser temperature particularly towards the cold end heat exchanger. This will reduce the driving buoyancy force for circulation and ultimately bring down the circulation rate. The fall in circulation may be observed in the C^*_{cf} curve of Fig. 5. The fall in circulation will again raise the hot stream exit temperature as depicted by 'BC' of the θ_{ho} plot in Fig. 5. The temperature profile along the loop length corresponding to point '*C*' ($\tau = 0.00188$) is shown in Fig. 6. One can appreciate a decrease in buoyancy force at this time interval compared to that at $\tau = 0.0016$.

The series of phenomenon observed between the points *A* and *C* represent a thermo-hydraulic cycle inside the loop. This cycle will start once again after '*C*'. However, the amplitude of the successive cycles will diminish at a faster rate so that after some time they will not be discernable. At $\tau = 0.003$ one can observe that the hot stream exit temperature and the circulation rate have attained nearly the steady state values. The temperature profile of the coupling fluid corresponding to this time step is shown in Fig. 6. The coupling fluid temperature values also confirm the attainment of steady state condition.

The development of the cold stream exit temperature needs a special attention. The cold stream exit temperature is observed to change from point '*D*'. The cold stream exit temperature will start responding only after a finite time delay ($\tau_d = 0.00132$) from the start of the transient. To have a better insight into this phenomena the temperature profile of coupling fluid at $\tau = 0.00132$ has also been recorded and depicted in Fig. 6.

The development of the thermal transport in the loop can be understood from the temperature curves at $\tau = 0.00036$ and 0.00132. In the first case, the effect of the temperature transient has reached only up to the end of the hot end heat exchanger. With the advancement of time, in the second case, this effect has reached up to the end of the riser. However, the cold end heat exchanger and the downcomer are still at the initial temperature of the loop. This is because the cold stream will start gaining energy effectively only after the warm fluid packet enters the CEHE. However, once the exit temperature of the cold stream starts changing, it will rise very fast as the circulation velocity is also increasing simultaneously at a faster rate. The maximum value of the cold stream exit temperature will correspond to the maximum circulation rate and the minimum value of the hot stream exit temperature as depicted in Fig. 5. After attaining the maximum value, the cold stream exit temperature will fall and eventually reach the steady state through a highly damped oscillation.

It is interesting to note that the time delay 'τ_d' for the response of cold stream is solely guided by the material advection. It is the time taken by a 'particle' of the coupling fluid to reach from the bottom of the riser (exit of the HEHE) to its top end (entry of the CEHE) just after the inception of the transient. Considering the motion of a fluid particle through the riser one may write

$$ds_{riser} = u_{cf}\,dt. \tag{24}$$

Therefore,

$$\int_0^{L_2} ds_{riser} = \int_0^{t_d} u_{cf}\,dt. \tag{25}$$

The above Eq. (25) may be written in the non-dimensional form

$$\int_1^{(1+K_1)} dS = \int_0^{\tau_d} C^*_{cf}\,d\tau. \tag{26}$$

Therefore,

$$K_1 = \int_0^{\tau_d} C^*_{cf}\,d\tau. \tag{27}$$

The value of τ_d obtained by numerical integration of Eq. (27), exactly matches with its value shown in Fig. 5.

The qualitative nature of the loop response as well as the responses of the cold and hot stream will not change much if modified ramp or modified exponential function is selected as the input transients. The dynamic behaviour of the loop in response to modified ramp and modified exponential excitation are depicted in Figs. 7 and 8, respectively. It may be noted that identical values of process parameters and steady state hot stream inlet temperature were selected for step, ramp and exponential excitations. This has resulted identical steady state responses from the loop fluid as well as from the hot and cold streams irrespective of the type of excitation. However, during the transient period the quantitative values of different responses depend on the type of excitation.

The initial rise of hot stream exit temperature closely follows the input excitation even in case of ramp and

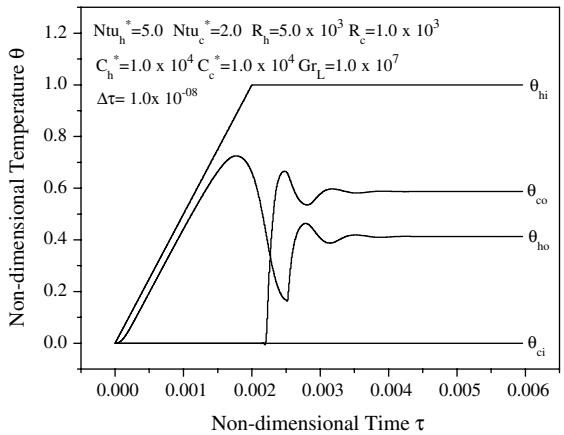

Fig. 7. Exit responses of hot and cold stream to modified ramp change in hot stream inlet temperature.

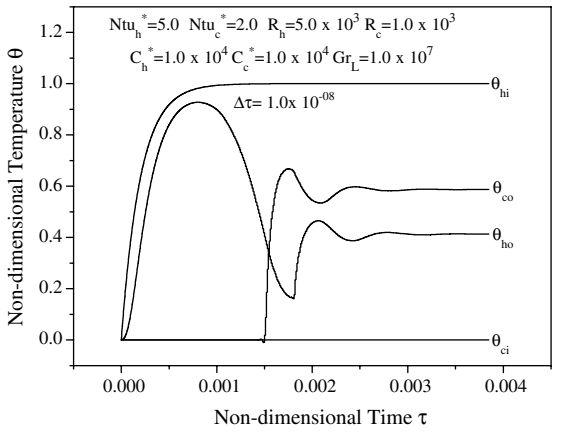

Fig. 8. Exit responses of hot and cold stream to modified exponential change in hot stream inlet temperature.

exponential inputs. However, the maximum value of the hot stream exit temperature is the highest in case of step input and lowest in case of ramp input during the initial transients. In case of step input the inlet temperature saturates to its final value instantaneously, the time delay for cold fluid exit temperature is the lowest in this case. Whereas it is observed that the time delay will be maximum in case of ramp input. Accordingly, the steady state condition for the coupling fluid as well as hot and cold streams will be achieved earlier in case of step input and longest time interval will be required to reach the steady state for the ramp input. This can be clearly observed from the variation of circulation rate for these three excitations depicted in Fig. 9. It may be noted that though the period of initial transients are different for different excitations the steady state values of circulation rate are identical for all the three excitations. Moreover,

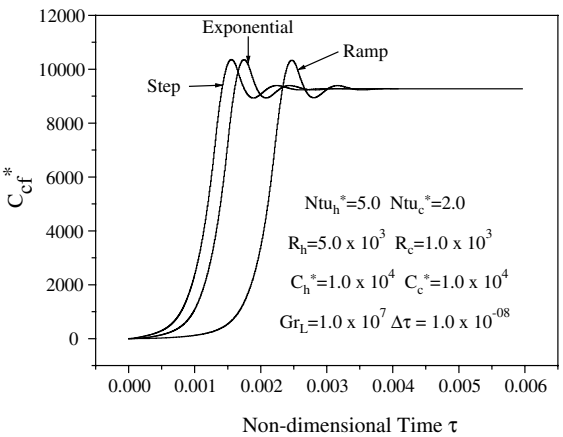

Fig. 9. Variation of circulation rate for step, modified ramp and modified exponential excitations.

the maximum and minimum values of the circulation velocities during the initial transient are also same in all the cases.

4.2. Sinusoidal excitation

The dynamic performance of the natural circulation loop due to an input sinusoidal excitation to hot fluid inlet temperature is qualitatively different from the loop response at other inputs as described above. As there is a continuous periodic change of input excitation, the temperature anywhere in the loop, in the cold and hot stream as well as the circulation rate in the loop will vary continuously. After the decay of the initial transients, these oscillations will become periodic. However, the amplitude and frequency of these periodic variations are functions of the input excitation.

Fig. 10a shows the variation of the exit temperatures of hot and cold streams for a relatively low frequency of

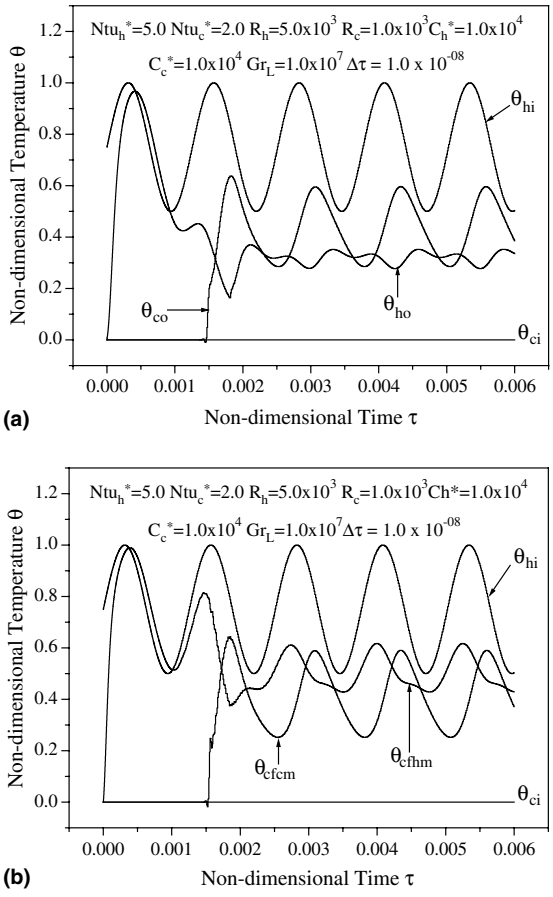

Fig. 10. Dynamic behaviour of the system for sinusoidal change in hot stream inlet temperature (lower frequency): (a) exit responses of hot and cold stream, (b) variation of coupling fluid temperature at the midpoint of heat exchangers.

input excitation. Fig. 10b depicts the variation of the coupling fluid temperatures at the midpoints of the hot and cold heat exchangers for the same condition. At the start of the transient the hot fluid exit temperature rapidly raises from its initial value of zero and closely follows the input sinusoidal excitation for a short while; then with some oscillation the temperature decreases to a minimum value. Gradually, the exit temperature attains a periodic nature through an oscillation. Initial rise and subsequent fall in the hot stream exit temperature was also observed in case of step, ramp and exponential excitations. However, in the present case the sinusoidal input makes this initial response more complex and oscillatory. It is interesting to note that, the response of the hot stream exit temperature during steady state does not represent a pure sinusoidal curve. Presence of more than one frequency is clearly observed. This is due to the complex interaction between the input excitation and the oscillatory flow inside the loop.

The cold fluid exit temperature starts responding to the sinusoidal excitation of hot stream inlet temperature only after a time delay. After the initial rise, the cold fluid exit temperature follows more or less a sinusoidal pattern. As there is no separate excitation for the cold stream, its response is guided primarily by the dynamic behaviour of the loop.

Fig. 10b shows the temperature variation of the coupling fluid at two opposite points in the horizontal portion of the loop. This also gives an idea of local temperature variation inside the loop at any particular instant of time. The temperature at midpoint of hot end heat exchanger is always higher than that of the hot stream exit temperature, but the nature of the variation of the former is different from that of the later. Whereas the temperature of the coupling fluid at the middle of the cold end heat exchanger closely follows that of cold stream exit temperature and its value is marginally lower than the cold stream exit temperature. The qualitative difference of the two periodic temperature curves depicted in Fig. 10b is obvious. At the HEHE the oscillations of the coupling fluid temperature is not purely sinusoidal whereas it is sinusoidal at the CEHE. Also, there is a phase difference between the peaks of these two curves. This difference induces an oscillatory flow through the loop. Moreover, these two curves indicate that not only the instantaneous values of the temperature vary along the loop, their nature of oscillations also varies locally.

Next, an effort has been made to study the loop performance with an increased frequency of sinusoidal excitation. The results have been shown in Fig. 11a and b. After the initial rise, the hot stream exit temperature exhibits a sinusoidal excitation for a short duration. However, the amplitude of the oscillation is lower compared to the input signal and there is a phase difference between these two. Subsequently, there is a fall in the hot stream exit temperature. Through an oscillatory behaviour it reaches its steady periodic nature. The cold stream outlet temperature starts responding after a time delay. It increases and through some oscillations it attains its steady periodic nature. However, one can observe a few distinct differences in the dynamic response of the loop due to the change of frequency of the input excitation. If Figs. 10a and 11a are compared one can clearly observe that with the increase of input frequency more time is required to reach the steady state. Moreover, at higher frequency the hot stream exit temperature also exhibits a sinusoidal nature. In Fig. 11b, the coupling fluid temperatures at the midpoints of hot and cold end heat exchangers also exhibit the steady periodic behaviour of sinusoidal nature after the decay of the initial transients. There is also a phase shift like the previous case (Fig. 10b). However, a reduction in amplitude for both the signals due to an increase in input frequency is obvious.

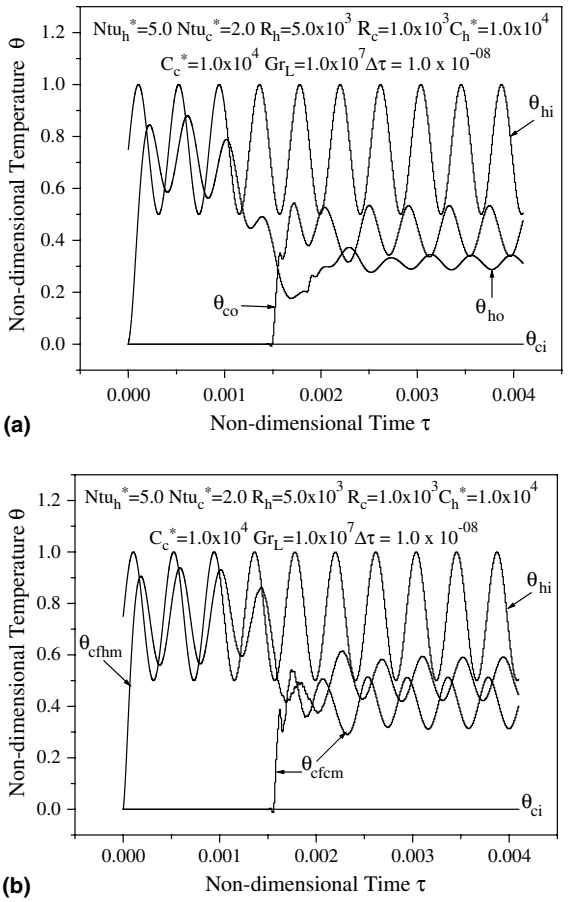

Fig. 11. Dynamic behaviour of the system for sinusoidal change in hot stream inlet temperature (higher frequency): (a) exit responses of hot and cold stream, (b) variation of coupling fluid temperature at the midpoint of heat exchangers.

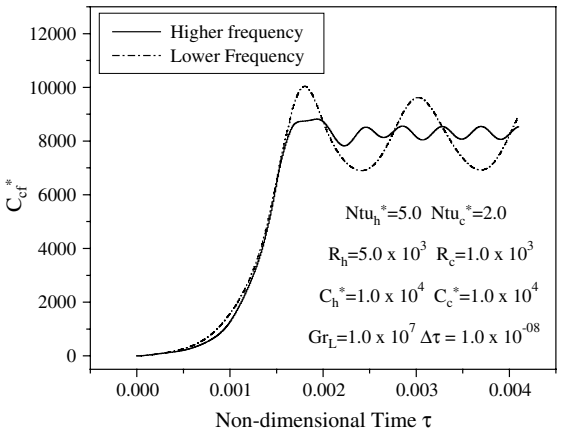

Fig. 12. Variation of circulation rate for sinusoidal change in hot stream inlet temperature.

In Fig. 12 the variation of circulation rate in response to sinusoidal excitation are depicted for the two different frequencies considered earlier. After the initial rise of the circulation rate in both the cases the loop exhibits a steady state sinusoidal fluctuation in circulation velocity. However, the amplitude of fluctuation is lower and the time taken to reach the steady state is higher at the high frequency. Therefore, Fig. 12 also corroborates the observations of Figs. 10 and 11.

5. Conclusion

In the present study, the dynamic response of a NCL with end heat exchangers has been studied numerically. The one-dimensional transient conservation equations; mass, momentum and energy for the loop fluid and energy for the hot and cold fluid streams have been solved through a finite element simulation for the imposed excitations to the hot stream inlet temperature. This inlet temperature is subjected to step, modified ramp, modified exponential and sinusoidal excitations. The ramp and exponential excitations are modified such that their maximum value is fixed a priori and is identical to the step function selected. For all these excitations the response of cold stream outlet temperature at the exit of the cold end heat exchanger has been studied. For the step, ramp and exponential excitations, the exit temperature of the cold end heat exchanger starts responding after a period of initial delay. For all these cases some initial transients are observed in the response. The delay periods are different for different excitations and this is related to the time needed for material advection. However, the maximum and minimum values of temperatures during the initial transients are equal in all the cases.

The response due to sinusoidal excitations is qualitatively different from the rest of the cases. This response becomes periodic after the initial transients. As the frequency of input excitations increases, the delay time increases and the amplitude of response decreases. The nature of variation of the circulation rate is also identical.

References

[1] N.M. Rao, M. Mishra, B. Maiti, P.K. Das, Effect of end heat exchanger parameters on the performance of a natural circulation loop, Int. Comm. Heat Mass Transfer 29 (2002) 509–518.
[2] N.M. Rao, B. Maiti, P.K. Das, Pressure variation in a natural circulation loop with end heat exchangers, Int. J. Heat Mass Transfer 48 (2005) 1403–1412.
[3] N.M. Rao, B. Maiti, P.K. Das, Stability behaviour of a natural circulation loop with end heat exchangers, ASME J. Heat Transfer, in press.
[4] R.B. Holmberg, Heat transfer in fluid coupled indirect heat exchanger systems, ASME J. Heat Transfer (1975) 449–503.
[5] X. Luo, X. Guan, M. Li, W. Roetzel, Dynamic behaviour of one-dimensional flow multistream heat exchangers and their networks, Int. J. Heat Mass Transfer 46 (2003) 705–715.
[6] Ch. Na Ranong, W. Roetzel, Steady state and transient behaviour of two heat exchangers coupled by a circulating flowstream, Int. J. Thermal Sci. 41 (2002) 1029–1043.
[7] P.J. Heggs, C.L. Render, Transient response of heat exchangers with one infinite capacitance fluid, Heat Transfer Eng. 4 (2) (1983) 19–27.
[8] F.E. Romie, Transient response of the counterflow heat exchanger, ASME J. Heat Transfer 106 (1984) 620–626.
[9] F.E. Romie, Transient response of the parallel-flow heat exchanger, ASME J. Heat Transfer 107 (1985) 727–730.
[10] D.D. Gvozdenac, Analytical solution of transient response of gas-to-gas parallel and counterflow heat exchangers, ASME J. Heat Transfer 109 (1987) 848–855.
[11] G. Pagliarini, G.S. Barozzi, Thermal coupling in laminar flow double-pipe heat exchangers, ASME J. Heat Transfer 113 (1991) 526–533.
[12] W. Roetzel, Y. Xuan, Transient response of parallel and counterflow heat exchangers, ASME J. Heat Transfer 114 (1992) 510–512.
[13] W. Roetzel, Y. Xuan, Transient behaviour of multipass shell-and-tube heat exchangers, Int. J. Heat Mass Transfer 35 (3) (1992) 703–710.
[14] W. Roetzel, Y. Xuan, The effect of core longitudinal heat conduction on the transient behaviour of multipass shell-and-tube heat exchangers, Heat Transfer Eng. 14 (1) (1993) 52–61.
[15] M.A. Abdelghani-Idrissi, F. Bagui, L. Estel, Analytical and experimental response time to flow rate step along a counterflow double pipe heat exchanger, Int. J. Heat Mass Transfer 44 (2001) 3721–3730.
[16] R. Greif, Y. Zvirin, A. Metrol, The transient and stability behavior of a natural convection loop, ASME J. Heat Transfer 101 (1979) 684–688.

[17] Y. Zvirin, R. Greif, Transient behaviour of natural circulation loops: two vertical branches with point heat source and sink, Int. J. Heat Mass Transfer 22 (1979) 499–504.
[18] A. Mertol, R. Greif, Y. Zvirin, The transient, steady state and stability behavior of a thermosyphon with throughflow, Int. J. Heat Mass Transfer 24 (1981) 621–633.
[19] N.M. Rao, Investigations on buoyancy induced circulation loops, Ph.D. Thesis, Indian Institute of Technology, Kharagpur, 2002.